Journal of Food Engineering 166 (2015) 316–324

Contents lists available at ScienceDirect

Journal of Food Engineering

journal homepage: www.elsevier.com/locate/jfoodeng

Process optimisation of rotating membrane emulsification through the study of surfactant dispersions

David M. Lloyd *, Ian T. Norton, Fotis Spyropoulos

Centre for Formulation Engineering, School of Chemical Engineering, University of Birmingham, Edgbaston, Birmingham B15 2TT, UK

ARTICLE INFO

Article history:
Received 13 October 2014
Received in revised form 21 May 2015
Accepted 7 June 2015
Available online 19 June 2015

Keywords:
Membrane emulsification
Rotor–stator
Surfactant
Diffusion
Interfacial tension
Energy density

ABSTRACT

In this study, a rotating membrane emulsification setup incorporating a 6.1 μm pore diameter Shirasu porous glass membrane was used to produce oil-in-water emulsions. The processing conditions varied between 0.2 and 1.5 bar for the transmembrane pressure and shear rates at the membrane surface between 0.6 s^{-1} and 104.6 s^{-1} were generated. All emulsions consisted of 10 vol.% of sunflower oil stabilised by one of four different surfactants (Tween 20, Brij 97, lecithin and sodium dodecyl sulphate) of either 0.1 wt.% or 1 wt.% concentration. A novel approach for emulsification processing was introduced which incorporates high hydrophilic–lypophilic balance, non-ionic surfactants within the dispersed phase rather than the continuous phase. A reduction in droplet size by at least a factor of 3 for the same formulation can be achieved without significant hindrance on disperse phase flux. This therefore suggests a possible strategy for further process optimisation.

1. Introduction

Formulating dispersions of one liquid phase within another immiscible liquid (i.e. an emulsion) remains an important area of research since these are readily incorporated within many foods, pharmaceutical, agrochemical and cosmetic products. Commonly cited examples from within the food industry include ice cream, mayonnaise and salad dressings, all of which are supplied to a global marketplace in large quantities. As such, there is increasing focus on the development of emulsification processes either to deliver improved product characteristics (e.g. greater stability, increased flavour perception) or to match expectation of current product quality but in more sustainable manner (e.g. lower energy consumption). Emulsions require the use of a surfactant to stabilise the droplet interface and as such, selection of an appropriate one is a key consideration for producing a microstructure with the desired droplet size distribution.

There are two philosophies that can be adopted to create an emulsion. The majority of emulsification processes focus on the breaking down droplets into smaller entities through subjection to mechanical energy e.g. homogenisers, rotor–stator mixers, colloid mills. A number of disadvantages are associated with forming droplets in this way, primarily associated with a wide droplet size range due to non-uniform energy dissipation and low energy efficiency due to repeated droplet break up and re-coalescence (Joscelyne and Tragardh, 2000; Charcosset, 2009; Gijsbertsen-Abrahamse et al., 2004; Jafari et al., 2008). In the latter instance, surfactant concentration is often overcompensated in order to achieve favourable processing kinetics. It is widely accepted that surfactants are some of the most costly components within many formulations. Processes that require both excessive use of energy and costly ingredients are neither environmentally nor economically sustainable and thus attention is shifting towards alternative processes that can minimise their use. More recent approaches look to build up droplets individually and then add them to the continuous phase in a controlled manner until the desired volume fraction of the phase to be dispersed is obtained (Nakashima et al., 1991; Yuan and Williams, 2014). This is the basis of membrane emulsification in which droplets are produced at individual membrane pore outlets, only detaching when the force holding the droplet at the membrane surface (primarily interfacial tension) is overcome by a combination of forces determined by operating parameters such as transmembrane pressure (inertial) and shear (drag) as well as by the physical properties of the phases e.g. density difference (buoyancy) Peng and Williams, 1998; De Luca and Drioli, 2006. With careful operation of the membrane emulsification process, droplets can be eloquently crafted and as such narrow droplet size distributions are achievable which may improve functionality of an emulsion based product e.g. stability against Ostwald ripening or ensure uniform release rate of an active ingredient throughout the system

* Corresponding author.
E-mail address: DML066@bham.ac.uk (D.M. Lloyd).

http://dx.doi.org/10.1016/j.jfoodeng.2015.06.028
0260-8774/

(Kobayashi et al., 2003). In combination with this benefit, the energy consumption is at least an order of magnitude lower than when adopting a droplet break down approach (Gijsbertsen-Abrahamse et al., 2004; Schubert et al., 1997; Walstra and Smulders, 1998). With the current rising costs of energy and negative environmental consequences associated with excessive energy consumption, this therefore increases the appeal of low energy, sustainable processes such as membrane emulsification.

Up until now, a number of drawbacks associated with membrane emulsification have perhaps held back the process from being implemented industrially. It is widely documented that the primary limitation is the low dispersed phase flux achievable (Kukizaki and Goto, 2007; Vladisavljevic and Schubert, 2003). Attempts to maximise the flux through application of high pressure driving force lead either to coalescence (Lepercq-Bost et al., 2010) or jetting of the dispersed phase (Kobayashi et al., 2003; Pathak, 2011), both of which reduce the level of control on the droplet size produced. Alternatively, a pre-mix membrane emulsification approach is used in which a coarse emulsion is passed through a membrane to break down droplets within pore channels (Surh et al., 2008; Vladisavljevic et al., 2004; Nazir et al., 2011, 2013). Whilst higher fluxes are achievable due to the generally lower viscosity (than pure dispersed phase), the requirement of multiple passes to ensure droplet uniformity negatively impacts the time and energy savings in comparison to the conventional approach. Furthermore, it is likely that fouling will occur as the mixture of oil, water and surfactant is broken down within the internal structure of the membrane (Trentin et al., 2009). If one aimed to maximise the level of control over droplet formation (at the expense of high dispersed phase flux), the advantages of energy saving are lost due to the long operating time. It is therefore very difficult to produce small, mono-dispersed droplets at a rate that is competitive with current emulsion production technologies. The key to solving this challenge is by ensuring rapid adsorption of surfactant to ensure early droplet detachment and stabilisation of the interface against coalescence. However, conventional approaches lead to membrane coalescence in the majority of cases irrespective of the surfactant type(s) and concentrations used (Wagdare and Marcelis, 2010; Abrahamse et al., 2002).

The aim of this study is to investigate the coupled behaviour between the droplet size of oil-in-water (O/W) emulsions and either the applied transmembrane pressure or the shear rate for a range of surfactant systems. Furthermore, a novel approach to ensure the rapid adsorption of surfactant is presented namely through positioning high hydrophilic–lypophilic balance (HLB), non-ionic surfactants within the dispersed phase rather than their common positioning within the continuous phase. This is subsequently compared with a pre-mix membrane emulsification approach as well as a rotor–stator high shear mixer both in terms of the emulsion droplet size produced but also the rate of production. The study will further understanding of membrane emulsification, enabling process optimisation to reduce droplet size, energy and surfactant consumption whilst maximising production rate simultaneously.

2. Experimental

2.1. Materials

Oil-in-water (O/W) emulsions containing 10 vol.% (unless otherwise stated) of commercially available sunflower oil (SFO) were produced. The aqueous phase was passed through a reverse osmosis unit and then a milli-Q water system. The emulsions were stabilised by a single surfactant in each case. The surfactants investigated were Tween 20 (polyoxyethylene 20 sorbitan monolaurate, Sigma Aldrich), Brij 97 (polyoxyethylene 10 oleoyl ether, Sigma Aldrich), SDS (sodium dodecyl sulphate, Fisher Scientific) and hydrolysed lecithin (Cargill). These were either dissolved within the aqueous continuous phase (w) or organic dispersed phase (o). The concentrations are expressed as weight percentages of the whole emulsion system.

2.2. Setup and procedure

2.2.1. Rotating membrane emulsification (RME)

The experiments were performed using a tubular, hydrophilic SPG membrane of 6.1 μm mean pore size (SPG Technology Co. Ltd., Miyazaki, Japan). The membrane dimensions were 10 mm outer diameter and 45 mm length, corresponding to an effective membrane surface area of 14.1 cm^2. The wall thickness of the membrane was approximately 1 mm. The membrane was mounted on an IKA Eurostar digital overhead stirrer and positioned in the processing vessel. This vessel was interchangeable allowing for two different sizes (inner diameters 20 mm and 60 mm) to be used in order to vary the shear applied at the membrane surface (0.6–12.0 s^{-1} and 52.4–104.7 s^{-1}). This altered the amount of continuous phase within the vessel since the membrane had to be submerged during process operation. Emulsion batch sizes between 25 and 110 g were produced. The membrane rotational speed in each experiment was varied between 100 and 2000 RPM. The transmembrane pressure (TMP) was also investigated in the range of 0.2–1.5 bar (gauge).

The schematic of the RME equipment setup is shown within an earlier publication (Lloyd et al., 2014). For typical emulsification operation, the oil phase (or oil/surfactant blend) was introduced to the inside of the membrane tube at the beginning of the experiment with the opening of the dispersed phase valve. Pressurisation of the dispersed phase storage tank with compressed air enabled the oil to permeate through the membrane to the outer continuous phase. Once the required mass of oil was added, the experiment was stopped by closing the dispersed phase valve.

In the case of pre-mix rotating membrane emulsification, a TMP of 0.5 bar (gauge) was used along with a membrane surface shear rate of 6.0 s^{-1} (1000 RPM and 60 mm diameter vessel). An initial 20 vol.% sunflower oil in water emulsion stabilised by 1 wt.% Tween 20 was formed (denoted Pass 1) and then subsequently passed through the membrane three times into an equal volume of distilled water. Observation of the droplet size decrease with each pass could therefore be observed but not without inadvertently diluting the dispersed phase volume fraction each time (to a minimum of 2.5 vol.% after Pass 4).

2.2.2. High shear mixer (HSM)

Emulsions were also produced using a rotor–stator high shear mixer (Silverson, model L4RT with 21 and 22 mm impeller and screen diameter respectively and 1 mm diameter screen holes). The two phases were introduced within the 60 mm diameter vessel prior to emulsification. The emulsion batch size was 110 g in all experimental runs. The amount of energy input during processing was varied by altering the rotational speed of the impeller between 2000 and 10,000 RPM for 1.5 min, which roughly corresponds to the time required to add the dispersed phase during the membrane emulsification process at 0.5 bar.

2.3. Droplet size measurements

Droplet size distribution of all emulsion samples were measured using a Malvern Mastersizer (United Kingdom) with a hydro 2000 small volume sample dispersion unit. Droplet sizes were

expressed as volume weighted mean diameter ($d_{4,3}$) average of a triplicate of measurements. The error bars represent one standard deviation and where not visible are smaller than the symbols used.

2.4. Interfacial tension (IFT) measurements

Interfacial tension (IFT) values were measured using a goniometer Easydrop from Kruss (Germany). The pendant drop method was used to determine the interfacial tension at 20 °C between a droplet of dispersed (oil) phase formed from a 1.8 mm diameter needle within a cuvette containing the continuous (aqueous) phase. These measurements were taken over a period of 1800 s at 30 s intervals to acquire both initial and equilibrium interfacial tension values.

The goniometer was also used to observe dynamic droplet formation with 1 wt.% of Tween 20 (within either the continuous or dispersed phase). This was performed under a low (100 μL min^{-1}) and high (1000 μL min^{-1}) injection rate of dispersed phase to emulate the effect of changing the applied transmembrane pressure during emulsification. Images were extracted at timescales representing initial size upon previous droplet detaching (t = 0 s), a short arbitrary time afterwards (t = 0.5 or 1 s) and then finally the emergence of the droplet neck as it begins to detach from the needle (t = variable).

2.5. Energy consumption measurements

The energy consumed during process operation was calculated firstly by measuring the power draw using a commercially available plug-in energy meter (Plug in Energy Monitor PI-022, EMW, UK) at a given equipment rotational speed. Ten measurements were recorded whilst the membrane or impeller was fully submerged firstly within distilled water and then a 10 vol.% sunflower oil-in-water emulsion (these two systems represent the two extremes of viscosity at the start and end points of emulsification processing). Theoretically, the power draw will be higher in order to maintain the rotational speed within more viscous media, in this instance this was not observed since the viscosity differences were too subtle. As such, the values obtained were averaged to find the rate of energy consumption in Joules per second, which when multiplied by the processing time gives the energy consumed to operate the process.

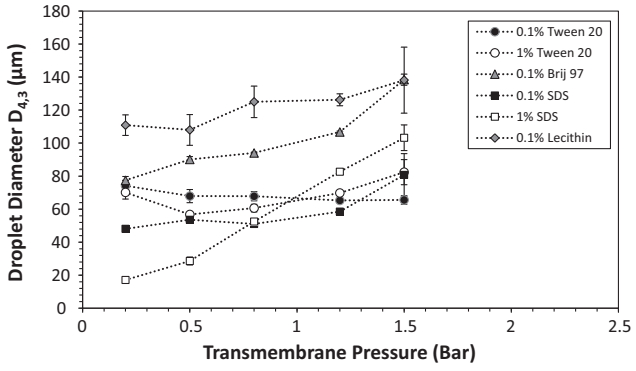

Fig. 1. The influence of transmembrane pressure on the mean droplet size for different surfactant types and concentrations. A membrane surface shear rate of 6.0 s^{-1} is applied corresponding to a rotational speed of 1000 RPM and a gap width of 25 mm.

3. Results and discussion

3.1. Effect of surfactant type

Fig. 1 shows the effect of transmembrane pressure (TMP) on the resultant droplet diameter for systems in which the surfactant is dissolved within the continuous phase. What is clear is that there is a variance in the behaviour of the trend between 0.2 and 1.5 bar depending on both the type of surfactant used and whether a low (0.1%) or high (1%) concentration is used.

For the low concentration systems, only Tween 20 exhibits a decrease across the pressure range investigated (from 74.2 μm to 65.6 μm). The systems containing Brij 97, SDS and lecithin follow a steady increase in droplet size with increasing pressure. This is expected in the absence of coalescence as more mass is transferred to the droplet during the detachment stage (Lloyd et al., 2014). What separates the behaviour of Tween 20 from the other surfactants can be explained by considering the chemical properties associated with each of the surfactants used. It would perhaps be expected that Brij 97 and Tween 20 would exhibit similar behaviour across the pressure range since they are both non-ionic surfactants with similar HLB values (12.4 and 16.9 respectively). However, the molecular weights of the two surfactants are considerably different with Tween 20 being much larger/heavier at 1228 g mol^{-1} compared to Brij 97 at 357 g mol^{-1}. Thus Brij 97 can move more freely throughout the bulk continuous phase towards the forming droplet interface due to less hydrodynamic resistance. On the other hand, Tween 20 is hindered by hydrodynamic resistance forces i.e. drag since it is larger and therefore is unable to adsorb as quickly to lower IFT and prevent coalescence. These suggestions are supported by the IFT values presented in Fig. 2a and b. As mentioned, since Brij 97 is a less effective surfactant (compared to Tween 20) at stabilising O/W emulsions as indicated by the HLB value, droplet diameters between 77.5 μm and 138.5 μm are formed which are larger than those observed with Tween 20. In addition, the use of ionic surfactants was also explored to consider the electrostatic effects on droplet formation. SDS is anionic with a high HLB value of approximately 40. This indicates it is an effective surfactant for stabilising forming oil droplets at the membrane surface and enabling detachment. A combination of electrostatic repulsive forces between adjacent forming droplets (that have adsorbed SDS molecules at their interface) and low IFT values (Fig. 2c) enabling droplets to detach earlier during formation virtually eliminate coalescence events and produce the smallest droplets (between 48.1 μm and 58.6 μm at a TMP $\leqslant$ 1.2 bar). Lecithin is different from the other systems as it is a zwitterionic phospholipid and has a low HLB value of around 5 (when hydrolysed). This indicates a preference to stabilise W/O emulsions rather than O/W produced in this case. A unique characteristic of lecithin is its ability to develop an elastic-like interface (Dimitrov et al., 1978) which may in turn prevent coalescence. The largest droplet diameters are formed (110.9–138.2 μm) since lecithin does not reduce the interfacial tension (IFT) to as great an extent as the other surfactants (Fig. 2). Furthermore, the rate of decrease is slow since the lecithin must first dissociate from vesicles formed in the bulk solution prior to adsorption at the forming droplet interface. This essentially lowers the effective concentration of free lecithin to stabilise the droplet since vesicle dissociation is the rate limiting step. Hence this combination of factors imply that droplets have to grow to much larger sizes in order to experience sufficient detachment force to overcome the higher retention forces (Spyropoulos et al., 2014). As a general observation, the droplet size average across the data set corresponds with the HLB value of the surfactant with higher values leading to smaller droplets as seen commonly within other

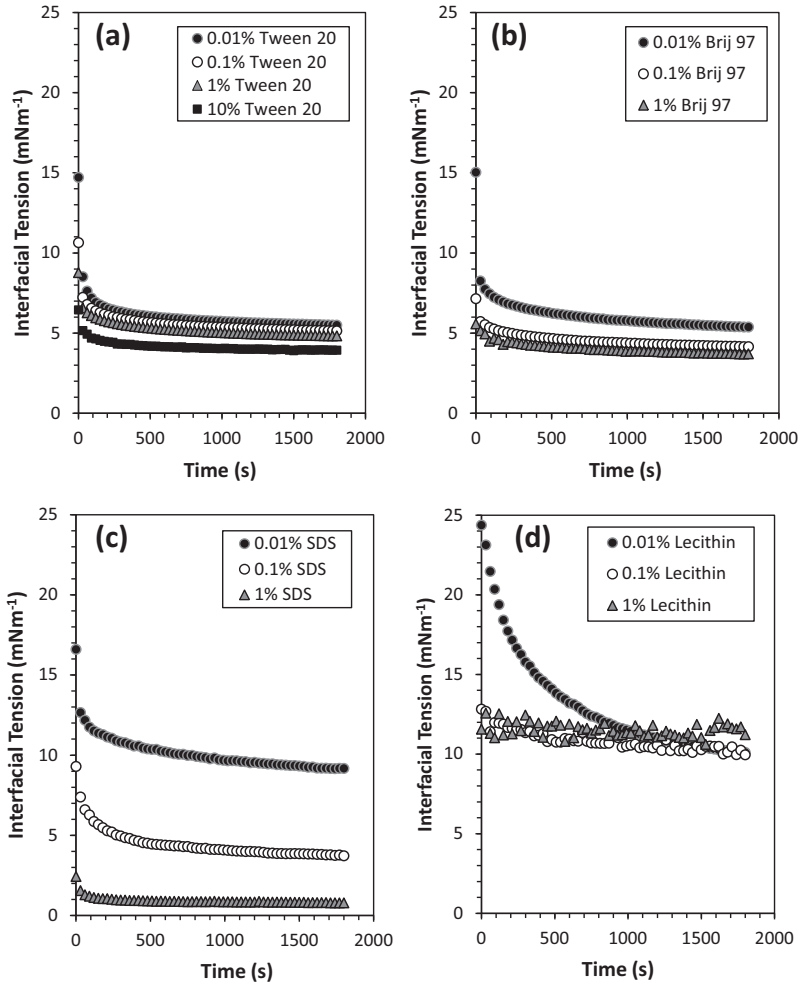

Fig. 2. Dynamic interfacial tension between sunflower oil and continuous phase containing variable concentration of surfactants: (a) Tween 20, (b) Brij 97, (c) SDS and (d) lecithin.

literature (Ban et al., 1994; Spyropoulos et al., 2011; Pawlik and Norton, 2013; Van der Graaf et al., 2004; Kukizaki, 2009).

Focussing on the high surfactant concentration systems, different behaviour is exhibited by the Tween 20 and SDS systems than was observed at 0.1 wt.%. It is expected that increasing surfactant concentration generally enables formation of smaller droplet sizes since there are more surfactant molecules available for adsorption and hence the IFT is lower (Schroder et al., 1998). For example, at 0.5 bar the droplet diameters of 0.1 wt.% and 1 wt.% of Tween 20 are 67.9 μm and 56.8 μm respectively. Similarly for SDS, these values are 53.6 μm and 28.6 μm respectively. However, there is a stark contrast in the behaviour of these systems across the pressure range. Tween 20 demonstrates a decrease followed by a plateau and then a slight increase which was not observed at the low concentration. The plateau region (known as the size-stable zone) is attributed to droplet formation due to a spontaneous transformation in its shape in order to lower its Gibbs free energy (Sugiura et al., 2001; Rayner et al., 2004). Such a phenomenon is more prevalent for high(er) IFT systems since they are more thermodynamically unstable. Therefore, with an increase in surfactant concentration to 1 wt.% and hence a lower IFT, the region in which this phenomenon potentially occurs becomes much narrower and so an eventual increase in droplet size upon further increase of TMP is observed as predicted previously (Lloyd et al., 2014). In the case of SDS, beyond 0.5 bar the droplet size increases extremely rapidly from 28.6 μm to 103.3 μm. Beyond 0.8 bar, the droplet sizes produced are larger than those formed at low concentration. It is therefore expected that there is a change in the droplet formation mechanism from dripping to jetting which is inherent to high pressures and low IFT systems (Sugiura et al., 2002). This suggests that whilst lowering the IFT is beneficial if one wanted to produce smaller droplets, it limits the ability to operate at higher throughputs of dispersed phase whilst still forming droplets in a controlled way i.e. through a dripping mechanism.

The effect of altering the shear rate at the membrane's surface (whilst applying a TMP of 0.5 bar) for different surfactant systems is shown in Fig. 3.

Generally, increasing the shear rate through higher rotational speeds or narrower gap sizes leads to formation of smaller droplet sizes because the drag and centrifugal detachment forces are greater so droplets detach earlier from the membrane surface. This will also occur if the IFT can be reduced to low values quickly so the magnitude of the interfacial tension force is smaller. It is therefore unsurprising that the 1 wt.% SDS system (which has the lowest IFT) produces the smallest droplet sizes between 27.5 μm and 58.2 μm followed by 0.1 wt.% SDS (49.3–89.5 μm) and 1 wt.% Tween 20 (57.0–94.1 μm). Furthermore, with higher rotational speeds which subsequently increase the continuous phase Reynolds and Taylor numbers, the transport of surfactant towards the interface is aided by a combination of diffusion and convection. As observed with the effect of TMP in Fig. 1, lecithin since it has a low HLB value produces the largest droplet sizes. The large error

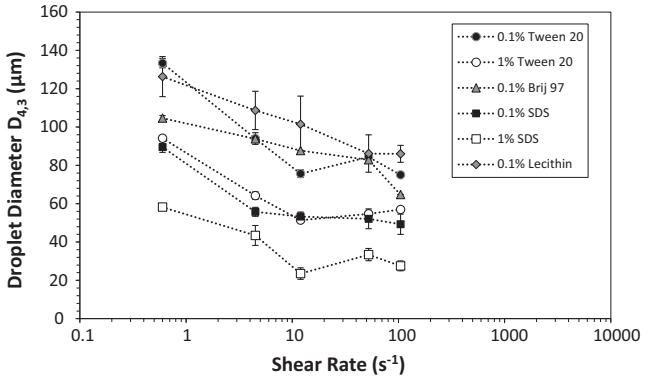

Fig. 3. The influence of membrane surface shear rate on the mean droplet size for different surfactant types and concentrations. A transmembrane pressure of 0.5 bar is applied.

bars when using lecithin indicate droplet formation is quite erratic. This may be perhaps due to variant effects that the shear has on deforming the elastic interface which may subsequently promote forms of droplet–droplet interactions (and therefore potentially coalescence) (Lepercq-Bost et al., 2010; Dragosavac et al., 2008; Egidi et al., 2008) or alter the velocity profile locally to the membrane surface (Timgren et al., 2009).

3.2. Effect of surfactant positioning

Within the previous section in which the surfactant was dissolved within the continuous phase, a wide range of droplet sizes was produced. Excluding SDS from this analysis, droplet sizes ranged from 51.4 µm to 138.5 µm. Given the pore diameter of the SPG membrane was 6.1 µm, this means the droplet size to pore size ratio varied between 8.4 and 22.8, which is at the upper end of ratio values suggested by other authors (Joscelyne and Tragardh, 2000; Charcosset, 2009). Since the hydrodynamics of the rotating membrane process are generally quite mild by comparison to a cross-flow membrane emulsification setup, the transport of surfactant to the forming droplet interface relies primarily on diffusion (and to a lesser extent convection). It can therefore be concluded that with the surfactant in the continuous phase, the transport and subsequent adsorption of surfactant is too slow and thus coalescence occurs in most cases. This is supported by observations within the work of Wagdare and Marcelis (2010) in which 4 wt.% Tween 20 and 1 wt.% SDS were unable to single-handedly prevent coalescence of sunflower oil droplets produced from a silicon nitride membrane. For SDS, the surfactant is able to stabilise droplet interfaces more effectively but is prone to jetting except under low TMP conditions where the pore fluid velocity is minimised. This raises two fundamentally important questions. Firstly, 'how can small droplets be produced quickly and in a controlled manner?' and similarly 'how can rapid adsorption of surfactant be ensured to minimise droplet coalescence in this process?'.

Interestingly, a recent article by Gassin et al. (2013) considered the effects of the transfer of amphiphilic molecules across an O/W interface on the IFT between the two phases. They supported earlier findings (Liggieri et al., 1997) suggesting that the IFT of a system could decrease below the equilibrium value at least in the initial stages depending on the partition coefficient of the surfactant and the kinetic rate to achieve adsorption equilibrium. This approach relies on surfactants that can be soluble in both aqueous and organic phases. Therefore, the use of non-ionic surfactants such as Tween 20 and Brij 97 and the zwitterionic surfactant lecithin are facilitated whilst SDS is excluded since it is insoluble in oil. It was hypothesised that by allowing surfactant to diffuse through a forming droplet interface during membrane emulsification, this would cause earlier detachment of droplets due to lower than expected IFT values whilst simultaneously limiting coalescence by enhancing the rate of adsorption. Thus, emulsion formation through membrane emulsification would be operated much more efficiently.

Fig. 4 shows the effect of where the surfactant is positioned on the resultant emulsion droplet size. Significant differences in the droplet size produced can be seen with much smaller emulsion droplets produced when the surfactant is blended with the dispersed phase. For example, emulsions formed by using 0.1 wt.% Tween 20 and Brij 97 positioned within the oil phase (o) are at least 3 times smaller than those formed with these surfactant conventionally placed within the aqueous phase for the same formulation/processing conditions. In this case, the droplet size to pore size ratio is much lower than previously observed, between 2.2 and 3.7. With 1 wt.% Tween 20 (o) and 0.2 bar TMP, a ratio as low as 1.1 is achieved. Furthermore, 0.1 wt.% Tween 20 (o) produces smaller droplets than a higher concentration of surfactant (1 wt.%) within the continuous phase (w). These two surfactants preferentiate towards being within the water phase, and so by diffusing out of the oil droplet to move into an aqueous environment, the IFT is seen to drop below the equilibrium value as shown by Fig. 5a. As an example, the IFT of 0.1 wt.% Tween 20 (o) reaches 1.7 mN m^{-1} after 30 min but when placed within the water phase (Fig. 4a) the value is 5.1 mN m^{-1} after the same time. It is anticipated that if left for a long enough period, the IFT values of the systems will converge to the same point. However, the RME process relies on droplet formation and detachment within a timescale <<2 s (in which the two phases are introduced) and thus a rapid decrease in IFT is beneficial. In the case of lecithin, this surfactant partitions in favour of being within the oil phase and is therefore 'reluctant' to diffuse out of the droplet and stabilise the forming interface. As a consequence, emulsions formed with lecithin in oil destabilised almost immediately most likely due to significant coalescence at the membrane surface. In terms of the effects of TMP, little variation is seen between 0.2 and 1.5 bar when Tween 20 and Brij 97 are positioned within the oil phase (<9 µm). Since the timescale for droplet formation and detachment is likely to be much shorter (since the droplets are smaller), any variations within dispersed phase flow will not drastically alter the volume contributed to each droplet during its detachment (Peng and Williams, 1998). For these systems, jetting does not occur because although the IFT is low, the slight increase in viscosity from blending 0.1 or 1 wt.% of surfactant into the 10 vol.% dispersed phase rather than the 90 vol.% of continuous phase leads to a lower dispersed phase pore fluid velocity such that the jetting point is not

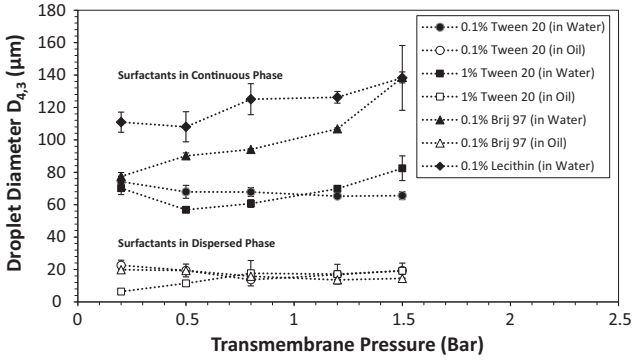

Fig. 4. The influence of transmembrane pressure on the mean droplet size for different surfactant positions. A membrane surface shear rate of 6.0 s^{-1} is applied corresponding to a rotational speed of 1000 RPM and a gap width of 25 mm.

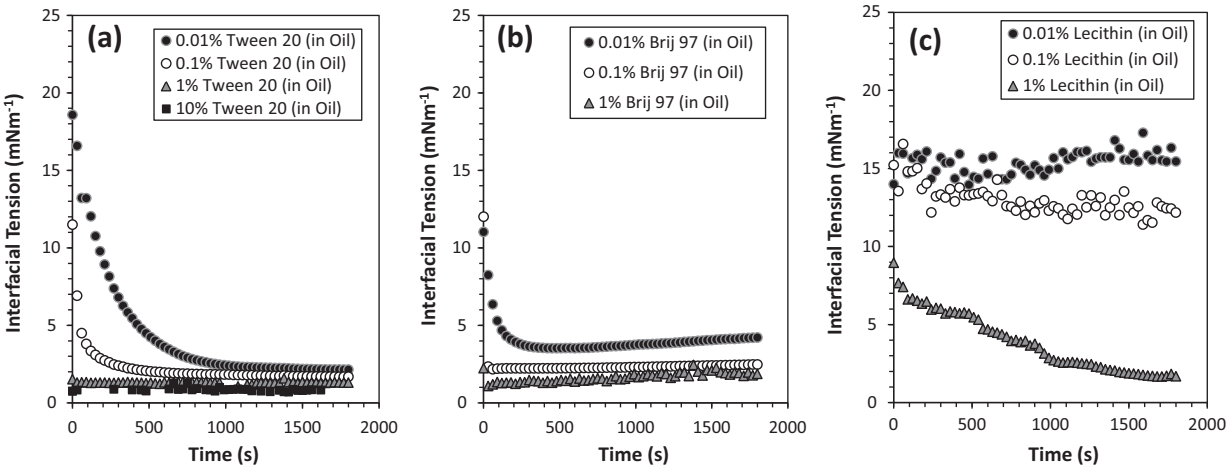

Fig. 5. Dynamic interfacial tension between distilled water and sunflower oil containing variable concentration of surfactants: (a) Tween 20, (b) Brij 97, (c) lecithin.

reached. It is likely that further increases in TMP beyond 1.5 bar would eventually result in the occurrence of droplet formation through jetting.

The effect of shear rate at the membrane surface on droplet diameter when considering the surfactant position is presented in Fig. 6.

Since the IFT of the non-ionic surfactant systems within oil is much lower than when in water, droplets are less resistant to shear and therefore detach earlier as smaller sizes. Only a small decrease is seen with increasing shear rate from 0.6 s^{-1} to 104.7 s^{-1}. For example, when using 0.1 wt.% Brij 97 (o), the droplet size varies between 15.2 μm and 21.5 μm (6.3 μm increase) compared to when the surfactant is placed within the aqueous phase (64.8–104.6 μm; 39.8 μm increase). This emphasises that if the aim is to produce small droplet diameters, this can be achieved using less surfactant and less energy input if operating under minimal shear rates with Tween 20 or Brij 97 within the dispersed phase. This conclusion is also supported by Fig. 7 in which images were captured of droplet formation for low (100 μl min^{-1}) and high (1000 μl min^{-1}) injection rates under quiescent continuous phase conditions (i.e. zero shear). Small droplets can be produced from the needle (representative of a pore channel) with 1 wt.% Tween 20 (o) and a low injection rate applied (Fig. 7b). In this case, the droplet detaches almost simultaneously as it forms since buoyancy overcomes the low IFT holding the droplet at the needle outlet. With a rotating membrane setup, the drag and centrifugal forces will inevitably lead to an even earlier detachment but perhaps reduce the extent of the size difference between the systems. To paraphrase, it is hypothesised that if the membrane surface shear rate was increased to much greater values than 104.7 s^{-1}, the droplet size difference between the observed systems may be minimal. However, care is required when selecting operating parameters such as the applied TMP and shear rate in conjunction with inherent system properties such as IFT and viscosity as can be seen in Fig. 7d in which the disperse phase is injected as a jet of liquid with less controlled droplet formation occurring downstream and out of visual range.

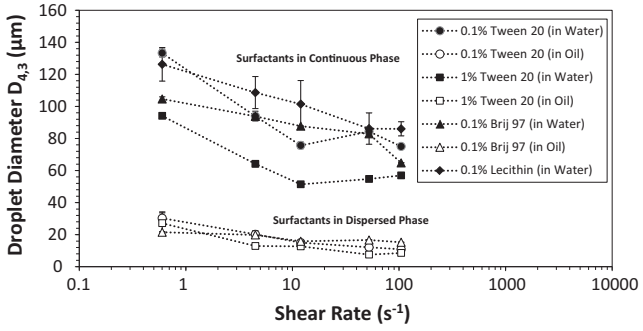

Fig. 6. The influence of membrane surface shear rate on the mean droplet size for different surfactant positions. A transmembrane pressure of 0.5 bar is applied.

3.3. Pre-mix rotating membrane emulsification

A number of publications have altered the approach of membrane emulsification by passing coarse emulsions through the membrane rather than a pure dispersed phase (Surh et al., 2008; Vladisavljevic et al., 2004; Nazir et al., 2011, 2013). This has led to additional benefits being cited such as high dispersed phase flux and lower energy consumption for producing high volume fraction emulsions (Nazir et al., 2010). The logic underlining this approach is that droplets upon leaving pore outlets are already stabilised by the surfactant provided for the formation of the initial coarse emulsion and therefore nullifies coalescence effects. If this is the case, this logic would also be valid with the surfactant being supplied within the dispersed phase as discussed in the previous section. To test this hypothesis, an initial emulsion of 20 vol.% dispersed phase was formed either with Tween 20 within the continuous phase (w) or dispersed phase (o) using the conventional membrane emulsification approach. Each of these emulsions was then passed through the same, cleaned membrane into distilled water a further three times to observe the extent of droplets being broken down within the pore channels and the obtained results are presented in Fig. 8.

As previously shown, the initial emulsion droplet size (Pass 1) is lower with the Tween 20 in the dispersed phase due to the partitioning behaviour of the surfactant. What is interesting is the extent and rate of droplet size minimisation upon passing the emulsions through the membrane repeatedly (Passes 2–4). With the surfactant placed within the oil phase, the droplets experience only a negligible reduction in size beyond applying a single pass. Using 1 wt.% Tween 20 (o) as an example, the initial droplet size of 15.4 μm is broken down to 6.1 μm, 4.5 μm and 4.3 μm upon applying further passes. If compared with 1 wt.% Tween 20 (w), the break down is much more prominent from 58.8 μm to 15.1 μm, 6.7 μm and 5.9 μm. With further passes, it is likely that the systems will achieve the same droplet size value. Furthermore, a much more efficient adsorption of surfactant is

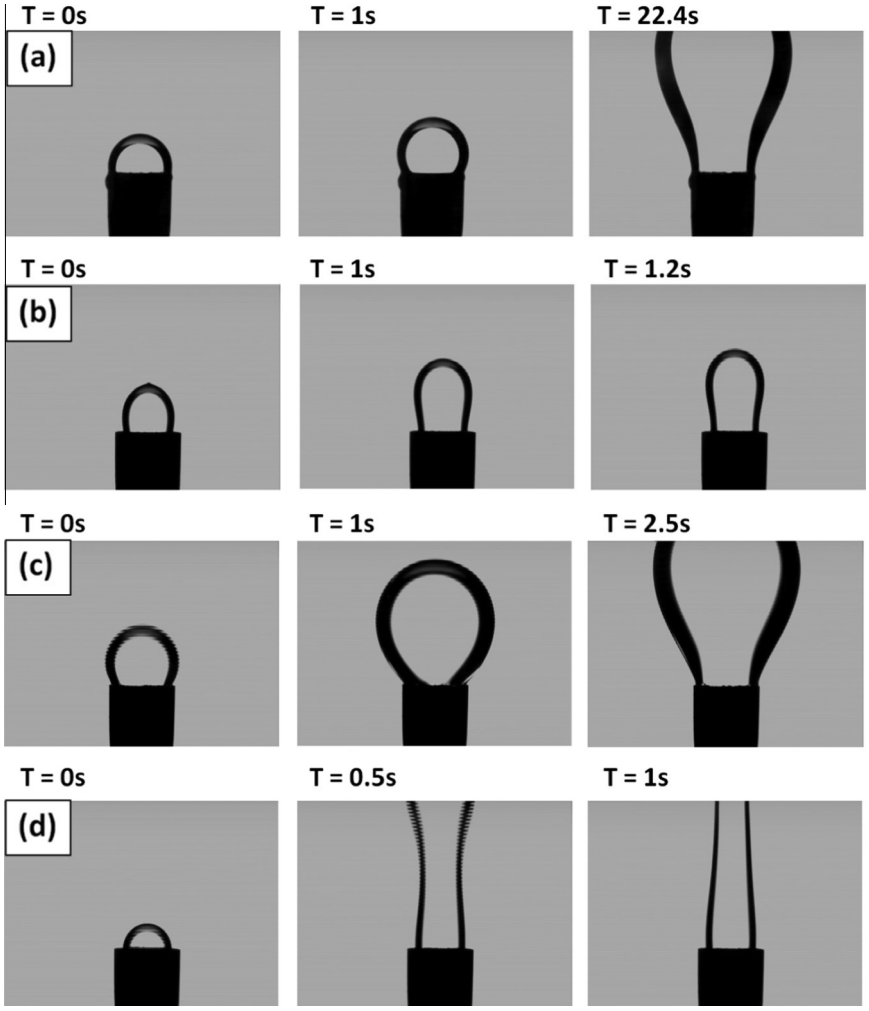

Fig. 7. Images of droplet formation and initial detachment stages from a 1.8 mm diameter needle under quiescent continuous phase conditions. Sunflower oil, water and 1 wt.% Tween 20 were used in all cases. The surfactant positioning and injection rate between low (100 μl min^{-1}) and high (1000 μl min^{-1}) were varied as follows: (a) low & in water, (b) low & in oil, (c) high & in water, (d) high & in oil.

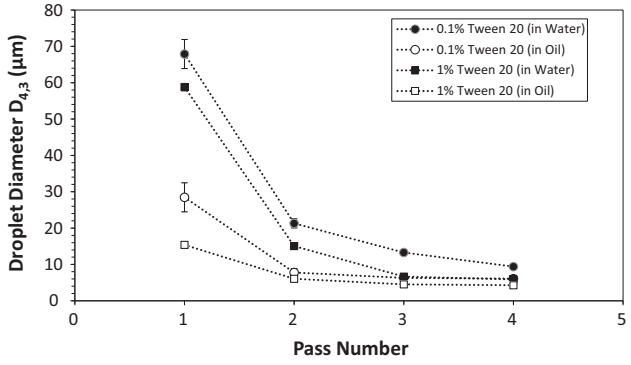

Fig. 8. The influence of pass number on the mean droplet size using sunflower oil, distilled water and 1 wt.% Tween 20. Pass 1 denotes the initial emulsion droplet size adopting the conventional approach. Pass 2–4 denotes the extent of droplet break down as the initial emulsion is passed through the membrane repeatedly. A transmembrane pressure of 0.5 bar and a membrane surface shear rate of 6.0 s^{-1} is applied in all cases.

achieved as demonstrated by 0.1 wt.% Tween 20 (o) reaching smaller diameters than 1 wt.% in the water phase. The point is, through applying the surfactant within the oil phase, the need of multiple passes to achieve sufficient break down to the minimum droplet size is eliminated. In fact, the very nature of adopting a pre-mix setup can be questioned since fouling is a severe problem as shown in Fig. 9.

In order to compare flow behaviour between the dispersed phase systems used (pure SFO, oil with surfactant and a

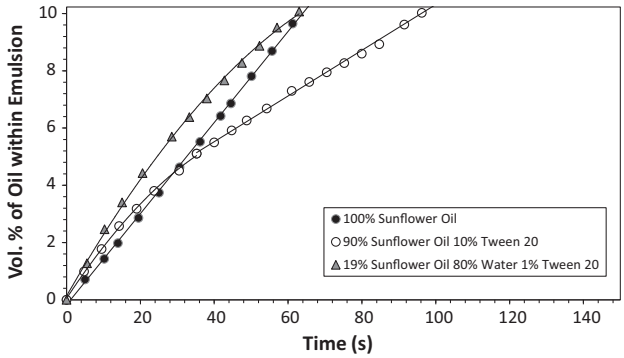

Fig. 9. Rate of oil addition during process operation at a transmembrane pressure of 0.5 bar and a membrane surface shear rate of 6.0 s^{-1} to produce an oil-in-water emulsion. The percentages represent the mass composition of the dispersed phase only. *Note:* the 90% sunflower oil and 10% Tween 20 data set is representative of 1 wt.% Tween 20 (o) systems above.

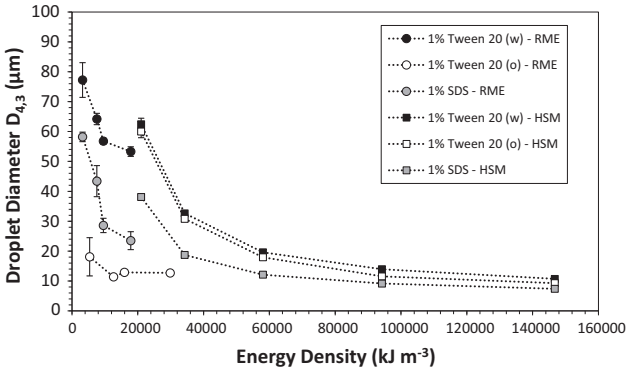

Fig. 10. The energy density utilised to produce emulsions containing 10 vol.% sunflower oil at a rate between 3.7 kg h^{-1} and 6.2 kg h^{-1} (depending on dispersed phase viscosity). The following notation is used: (w) surfactant in water, (o) surfactant in oil, (RME) Rotating Membrane Emulsification, (HSM) High Shear Mixer.

pre-emulsion), Fig. 9 is expressed as volume fraction of oil added to the final emulsion since the objective is to reach a pre-defined quantity of this material. There is no doubt that the flux of a pre-emulsion is much higher than of pure oil but a significant volume of that emulsion must pass through the membrane to arrive at the end point of the process. What is apparent is that the rate of mass transfer/addition for the pre-emulsion is not linear – that would be expected by Darcy's law. This suggests an increase in resistance to flow over time which is likely to be caused by fouling. In the case of droplets slightly larger in diameter than the membrane pore channel, the shear exerted within the internal structure may not be great enough to overcome the droplet Laplace pressure. As a consequence, the droplet cannot deform sufficiently enough to pass through and thus it becomes trapped within the membrane, causing a blockage. However, much larger droplets will be broken up by the shear within the pore channel whilst smaller droplets will pass through unopposed. The flow behaviour of pure SFO in contrast to a pre-emulsion obeys a linear addition of material over time whilst a mixture of SFO and Tween 20 exhibits a slight reduction in the rate followed by a linear region. The surfactant may perhaps coat the membrane walls within pore channels during the initial stages of operation (and hence the flow behaviour) before the mixture starts acting as a bulk material. As expected the gradient of this linear region is lower than pure SFO since the viscosity is higher. With the requirement to pass the pre-emulsion through the membrane further times to achieve sufficient break down of droplets, it may be therefore more efficient to operate using a dispersed phase with lower flux but which ensures rapid adsorption of surfactant from a single pass i.e. using high HLB non-ionic surfactant within the oil.

3.4. Energy efficiency

Finally, the energy density to form emulsions containing 10 vol.% of oil dispersed phase is considered at production rates varying between 3.7 kg h^{-1} and 6.2 kg h^{-1}. This is with respect to where the surfactant is positioned for both the RME process but also a rotor–stator HSM.

As can be seen in Fig. 10, there are fundamental differences between the processes both in terms of the energy consumed but also the behaviour of the systems investigated. Applying more energy through the rotation of the membrane or the impeller leads to formation of smaller droplets by enabling detachment/droplet break down. Generally, RME produces emulsions with at least one order of magnitude less energy but within most other literature, at the expense of either droplet size or rate of production. What is significant is that ensuring rapid adsorption of surfactant by positioning the Tween 20 within the oil phase (o) results in droplet size ranges produced that are similar to those produced with high shear processing (around 12.7–18.1 μm) but with much less energy (between 4600 and 30,100 kJ m^{-3} for RME compared to 33,400–147,000 kJ m^{-3} for HSM). Focussing on the HSM process, the differences of where the surfactant is positioned on droplet size are almost negligible. In this process, droplets are continuously broken down during operation and as such, mechanically induced convection rather than diffusion forces the IFT to equilibrium value. The effect of an initial decrease in IFT below equilibrium and the subsequent advantages in terms of facilitating droplet break down are therefore lost at the early stages of processing. Due to the variation in the approach by which droplets are formed, SDS appears a more appropriate surfactant during HSM processing since the electrostatic repulsion between droplet interfaces prevents re-coalescence within the continuous phase. Droplets can reach a minimum size of 7.4 μm at 10,000 RPM compared to 10.7 μm and 9.3 μm for Tween 20 (w) and Tween 20 (o) respectively. Additionally, the high HLB value and low equilibrium value of IFT allows for further reduction in droplet Laplace pressure and facilitates droplet break down. However, SDS is not as effective during the RME process since Tween 20 can achieve lower IFT values when it diffuses out of the droplet (below 0.9 mN m^{-1}). Moreover, supplying surfactant in this way ensures it is provided at a rate proportional to the dispersed phase flow rather than being depleted from the continuous phase over time i.e. as it is needed. Whilst the production rate is reduced due to the increase in dispersed phase viscosity, the advantages in energy consumption and thus processing efficiency are still maintained.

4. Summary and conclusions

The effects of transmembrane pressure and shear rate have been investigated for four different surfactants and variable concentrations using a rotating membrane emulsification setup. In this work, a novel approach in which surfactant is provided via the dispersed phase, rather than its conventional positioning within the continuous phase was introduced. By allowing material to diffuse through the interface, this leads to a reduction in interfacial tension below the equilibrium value which is highly beneficial to the membrane emulsification process in order to prevent coalescence and allow early droplet detachment. However, this approach has only been successfully demonstrated for stabilising O/W droplets using high HLB non-ionic surfactants such as Tween 20 and Brij 97. When using a low HLB surfactant such as lecithin, droplets were not stabilised. Due to the partition coefficient of the lecithin used, this surfactant remains primarily within the oil phase and hence does not diffuse out of the droplet to the extent of the high HLB surfactants. Membrane emulsification with surfactant within the dispersed phase compares favourably to a pre-mix emulsification setup since droplet size minimisation that is achieved through multiple passes, is in this case obtained much earlier by ensuring rapid adsorption of the surfactant. Furthermore, the effects of membrane fouling are avoided at least during short term process operation although long term effects on the dispersed phase flux are currently unknown. By considering the positioning and type of surfactant, membrane emulsification can be competitive with a rotor–stator high shear mixer in terms of droplet size and production rate whilst still being favourable in terms of energy consumption by at least an order of magnitude. An expansion of this study would be to investigate a wider variety of surfactants beyond Tween 20, Brij 97 and lecithin as well as to observe whether advantages using this approach are upheld at higher dispersed phase volume fractions or a larger scale.

References

Abrahamse, A.J., van Lierop, R., van der Sman, R.G.M., van der Padt, A., Boom, R.M., 2002. Analysis of droplet formation and interactions during cross-flow membrane emulsification. J. Membr. Sci. 204 (1–2), 125–137.

Ban, S., Kitana, M., Yamasaki, A., 1994. Preparation of O/W emulsions with poly(oxyethylene) hydrogenated castor oil by using SPG membrane emulsification. Nippon Kagaku Kaishi 8, 737–742.

Charcosset, C., 2009. Preparation of emulsions and particles by membrane emulsification for the food processing industry. J. Food Eng. 92 (3), 241–249.

De Luca, G., Drioli, E., 2006. Force balance conditions for droplet formation in cross-flow membrane emulsifications. J. Colloid Interface Sci. 294 (2), 436–448.

Dimitrov, D.S., Panaiotov, I., Richmond, P., Ter-Minassian-Saraga, L., 1978. Dynamics of insoluble monolayers. J. Colloid Interface Sci. 65, 483–494.

Dragosavac, M.M., Sovilj, M.N., Kosvintsev, S.R., Holdich, R.G., Vladisavljevic, G.T., 2008. Controlled production of oil-in-water emulsions containing unrefined pumpkin seed oil using stirred cell membrane emulsification. J. Membr. Sci. 322 (1), 178–188.

Egidi, E., Gasparini, G., Holdich, R.G., Vladisavljevic, G.T., Kosvintsev, R., 2008. Membrane emulsification using membranes of regular pore spacing: droplet size and uniformity in the presence of surface shear. J. Membr. Sci. 323 (2), 414–420.

Gassin, P., Champory, R., Martin-Gassin, G., Dufreche, F., Diat, O., 2013. Surfactant transfer across a water/oil interface: a diffusion/kinetics model for the interfacial tension evolution. Colloids Surf. A 436, 1103–1110.

Gijsbertsen-Abrahamse, A.J., van der Padt, A., Boom, R.M., 2004. Status of cross-flow membrane emulsification and outlook for industrial application. J. Membr. Sci. 230 (1–2), 149–159.

Jafari, S.M., Assadpoor, E., He, Y., Bhandari, B., 2008. Re-coalescence of emulsion droplets during high-energy emulsification. Food Hydrocoll. 22 (7), 1191–1202.

Joscelyne, S.M., Tragardh, G., 2000. Membrane emulsification – a literature review. J. Membr. Sci. 169 (1), 107–117.

Kobayashi, I., Nakajima, M., Mukataka, S., 2003. Preparation characteristics of oil-in-water emulsions using differently charged surfactants in straight-through microchannel emulsification. Colloids Surf. A 229 (1–3), 33–41.

Kukizaki, M., 2009. Shirasu porous glass (SPG) membrane emulsification in the absence of shear flow at the membrane surface: Influence of surfactant type and concentration, viscosities of dispersed and continuous phases, and transmembrane pressure. J. Membr. Sci. 327 (1–2), 234–243.

Kukizaki, M., Goto, M., 2007. Preparation and characterization of a new asymmetric type of Shirasu porous glass (SPG) membrane used for membrane emulsification. J. Membr. Sci. 299 (1–2), 190–199.

Lepercq-Bost, E., Giorgi, M., Lsambert, A., Arnaud, C., 2010. Estimating the risk of coalescence in membrane emulsification. J. Membr. Sci. 357 (1–2), 36–46.

Liggieri, L., Ravera, F., Amodio, C., Miller, R., 1997. Adsorption kinetics of alkylphosphine oxides at water/hexane interface: 1. Pendant drop experiments. J. Colloid Interface Sci. 186 (1), 46–52.

Lloyd, D.M., Norton, I.T., Spyropoulos, F., 2014. Processing effects during rotating membrane emulsification. J. Membr. Sci. 466, 8–17.

Nakashima, T., Shimizu, M., Kukizaki, M., 1991. Membrane emulsification by microporous glass. Key Eng. Mater. 61–62, 513–516.

Nazir, A., Schroen, K., Boom, R., 2010. Premix emulsification: a review. J. Membr. Sci. 362 (1–2), 1–11.

Nazir, A., Schroen, K., Boom, R., 2011. High-throughput premix membrane emulsification using nickel sieves having straight-through pores. J. Membr. Sci. 383 (1–2), 116–123.

Nazir, A., Boom, R.M., Schroen, K., 2013. Droplet break-up mechanism in premix emulsification using packed beds. Chem. Eng. Sci. 92, 190–197.

Pathak, M., 2011. Numerical simulation of membrane emulsification: effect of flow properties in the transition from dripping to jetting. J. Membr. Sci. 382 (1–2), 166–176.

Pawlik, A.K., Norton, I.T., 2013. SPG rotating membrane technique for production of food grade emulsions. J. Food Eng. 114, 530–537.

Peng, S.J., Williams, R.A., 1998. Controlled production of emulsions using crossflow membrane Part I: droplet formation from a single pore. Chem. Eng. Res. Des. 76 (8), 894–901.

Rayner, M., Tragardh, G., Tragardh, C., Dejmek, M., 2004. Using the surface evolver to model droplet formation processes in membrane emulsification. J. Colloid Interface Sci. 279 (1), 175–185.

Schroder, V., Behrend, O., Schubert, H., 1998. Effect of dynamic interfacial tension on the emulsification process using microporous, ceramic membranes. J. Colloid Interface Sci. 202 (2), 334–340.

Schubert, H., 1997. Advances in the production of food emulsions, in: Proceedings of Engineering and Food at ICEF 7, ICEF-Conference, Academic Press, Brighton, pp. AA82–AA87.

Spyropoulos, F., Hancocks, R.D., Norton, I.T., 2011. Food-grade emulsions prepared by membrane emulsification techniques. Proc. Food Sci. 1, 920–926.

Spyropoulos, F., Lloyd, D.M., Hancocks, R.D., Pawlik, A.K., 2014. Advances in membrane emulsification. Part B: recent developments in modelling and scale-up approaches. J. Sci. Food Agric. 94 (4), 628–638.

Sugiura, S., Nakajima, M., Iwamoto, S., Seki, M., 2001. Interfacial tension driven monodispersed droplet formation from microfabricated channel array. Langmuir 17, 5562–5566.

Sugiura, S., Nakajima, M., Kumazawa, N., Iwamoto, S., Seki, M., 2002. Characterization of spontaneous transformation-based droplet formation during microchannel emulsification. J. Phys. Chem. B 106 (36), 9405–9409.

Surh, J., Jeong, Y.G., Vladisavljevic, G.T., 2008. On the preparation of lecithin-stabilized oil-in-water emulsions by multi-stage premix membrane emulsification. J. Food Eng. 89 (2), 164–170.

Timgren, A., Tragardh, G., Tragardh, C., 2009. Effects of pore spacing on drop size during cross-flow membrane emulsification – a numerical study. J. Membr. Sci. 337 (1–2), 232–239.

Trentin, A., Ferrando, M., Lopez, F., Guell, C., 2009. Premix membrane O/W emulsification: effect of fouling when using BSA as emulsifier. Desalination 245 (1–3), 388–395.

Van der Graaf, S., Schroen, C.G.P.H., van der Sman, R.G.M., Boom, R.M., 2004. Influence of dynamic interfacial tension on droplet formation during membrane emulsification. J. Colloid Interface Sci. 277 (2), 456–463.

Vladisavljevic, G.T., Schubert, H., 2003. Influence of process parameters on droplet size distribution in SPG membrane emulsification and stability of prepared emulsion droplets. J. Membr. Sci. 225 (1–2), 15–23.

Vladisavljevic, G.T., Shimizu, M., Nakashima, T., 2004. Preparation of monodisperse multiple emulsions at high production rates by multi-stage premix membrane emulsification. J. Membr. Sci. 244 (1–2), 97–106.

Wagdare, N.A., Marcelis, A.T.M., Boen Ho, O., Boom, R.M., 2010. High throughput vegetable oil-in-water emulsification with a high porosity micro-engineered membrane. J. Membr. Sci. 347 (1–2), 1–7.

Walstra, P., Smulders, P.E.A., 1998. Emulsion formation. In: Binks, B.P. (Ed.), Modern Aspects of Emulsion Science. The Royal Society of Chemistry, Cambridge, pp. 56–99.

Yuan, Q., Williams, R.A., 2014. Precision emulsification for droplet and capsule production. Adv. Powder Technol. 25 (1), 122–135.